Determination of the optimal acquisition protocol of breath-hold PET/CT for the diagnosis of thoracic lesions

Mitsumoto, Katsuhiko
Department of Health Sciences, Graduate School of Medical Sciences, Kyushu University

Abe, Koichiro
Department of Clinical Radiology, Graduate School of Medical Science, Kyushu University

Sakaguchi, Yuichi
Department of Health Sciences, Graduate School of Medical Sciences, Kyushu University

Zhang, Tiejiao
Department of Health Sciences, Graduate School of Medical Sciences, Kyushu University

他

出版情報：Nuclear Medicine Communications. 32 (12), pp.1148-1154, 2011-12. Lippincott Williams & Wilkins
バージョン：

TITLE:

Determination of the Optimal Acquisition Protocol of Breath-Hold PET/CT for the Diagnosis of Thoracic Lesions

Short title: Breath-Hold PET/CT for Thoracic Lesions

Katsuhiko Mitsumoto, BS[1], Koichiro Abe, MD, PhD[2], Yuichi Sakaguchi, MS[1], Tiejiao Zhang, MS[1], Yosuke Tachiya, BS[3], Nobuyoshi Ohya, PhD[3], Shingo Baba, MD, PhD[2], Masayuki Sasaki, MD, PhD[1]

1 Department of Health Sciences, Graduate School of Medical Sciences, Kyushu University

2 Department of Clinical Radiology, Graduate School of Medical Science, Kyushu University

3 Department of Medical Technology, Kyushu University Hospital

Corresponding author and reprint request to:

Masayuki Sasaki, MD, PhD

Division of Radiological Science, Department of Health Sciences, Graduate School of

Medical Sciences, Kyushu University

3-1-1 Maidashi, Higashi-ku, Fukuoka 812-8582, Japan

TEL: +81-92-642-6746, FAX: +81-92-642-6723

E-mail: msasaki@hs.med.kyushu-u.ac.jp

This study was supported in part by a Grant-in Aid for Scientific Research © from the Japan Society for the Promotion of Science KAKENHI (22611012).

Abstract

Objective: The aim of this study was to determine the optimal acquisition scan protocol for breath-hold (BH)-FDG-PET for the examination of thoracic lesions.

Methods: We studied 32 thoracic lesions in 21 patients. Whole-body PET/CT scanning with free breathing (FB) was performed for 3 minutes per bed position, followed by BH-PET/CT scanning 5 times for 20 seconds. Summed BH images with total acquisition times of 40, 60, 80 and 100 seconds were generated (BH×2, BH×3, BH×4 and BH×5, respectively). The displacements between PET and CT images, the lesion volume of the PET image, SUVmax and the quality of the PET image were assessed in relation to the clinical characteristics of each patient and the summation of the BH-PET images.

Results: BH-PET significantly decreased the tumor volume (FB: 7.23±9.70 cm^3, BH×5: 4.71±5.14 cm^3, P<0.01) and increased the SUVmax (FB: 6.27±5.41, BH×5: 7.53±6.28, P<0.01). The displacement between the PET and CT images was significantly improved in the BH scans (FB: 0.77±0.53 cm, BH×5: 0.36±0.24 cm, P<0.01). In addition, aging and the lung function of patients influenced the reproducibility of BH-PET/CT. The summed BH-PET images, obtained by summation of 3 or more BH-PET images (total acquisition time of 60 seconds or more), achieved good image quality**.**

Conclusion: BH-PET/CT improved the misregistration between PET and CT images and increased the SUVmax of thoracic lesions. The recommended number of BH-PET images for summation with 20 seconds of acquisition time is 3 or more.

Key words: PET/CT, breath-hold, thoracic lesion, respiratory motion, scan protocol

Introduction

The metabolic images obtained by ^{18}F-2-fluoro-2-deoxy-D-glucose (FDG) -positron emission tomography (PET) have been used for detecting, staging, restaging and monitoring the therapeutic response of non-small cell lung cancer (NSCLC) [1-5]. Recent developments in PET/ computed tomography (CT) technology have enabled us to acquire anatomical and metabolic information simultaneously, making it possible to obtain more accurate diagnoses than with PET alone [6, 7]. Although the system sensitivity of PET for detecting photons has been improved, PET emission data acquisition still requires a few minutes per bed position, and consequently, is performed with free breathing (FB). Therefore, PET images can lead to the overestimation of lesion volume and image blurring due to the respiratory motion. The standardized uptake value (SUV) of FDG-PET is decreased by respiratory motion [8, 9] and thus this decrease influences the diagnostic accuracy for malignancies, particularly in the case of thoracic lesions. Because the maximum SUV (SUVmax) is widely used for differentiating between benign and malignant lesions and for monitoring the therapeutic response of malignancies, an accurate measurement of the SUVmax is important for clinical assessment [10, 11]. Another problem is that a misregistration of the PET/CT fusion images often occurs because the CT images are a snapshot representing a short acquisition time.

Recently developed highly precise radiotherapy, such as stereotactic radiotherapy, has improved the outcome of patients with NSCLC [12]. Successful treatment is considered to be dependent on focusing a high radiation dose on the tumor and avoiding unnecessary irradiation to normal tissue. This method requires target immobilization and it is usually performed under breath-holding or a respiratory-gating system [13, 14]. Because precise treatment planning is necessary for the success of this method, the high diagnostic ability of PET/CT is expected to be useful for such treatment planning [11, 15].

Respiratory-gated PET/CT was developed to minimize the artifacts of respiratory motion during image acquisition [16, 17]. Both the PET and CT images obtained by dynamic acquisition with the cine mode are divided into several respiratory phases, and then PET/CT fusion images of each phase are generated. Although this protocol enables the improvement of the coregistration of fusion images and attainment of an accurate SUVmax, it requires long acquisition and postprocessing times. The dynamic CT scan also delivers a high radiation dose to the patient. For these reasons, the dynamic PET/CT technique has not been widely used.

Recently developed high-sensitivity PET scanners and 3D acquisition modes have enabled clinicians to obtain images within a short acquisition time [18, 19]. Breath-hold (BH)-PET/CT has been recommended for the diagnosis of thoracic lesions. This technique can be easily performed with short breath-holding without any specialized equipment. Some papers have already reported the usefulness of BH-PET/CT [20-27]. Although some authors have examined the scanning protocol by phantom studies [26-28], an appropriate scanning protocol has not yet been tested in the clinical setting.

In this study, our goal was to determine an appropriate scanning protocol for BH-PET/CT in relation to patient features and image quality of BH-PET.

Materials and methods

Patient characteristics

This study was approved by the review board of the Ethics Committee of our institution (No. 21-58). This study was retrospective in nature, and its results did not influence any further therapeutic decision-making. This study analyzed 21 patients with thoracic lesions. In our institution, patients whose thoracic lesions were found by a whole body PET/CT underwent a subsequent thoracic BH-PET/CT examination. The BH-PET/CT examination was performed in a total of 37 patients during the approved period. Among these patients, FDG positive lung lesions were observed in 21 patients, and these patients were analyzed in this study.

We studied 32 thoracic lesions in 21 patients (10 male and 11 female; mean and standard deviation (SD) of age 60.8±14.6 years; range: 21-86 y), including 26 malignant lesions and 6 benign lesions. Malignant lesions consisted of NSCLC (n=2), and metastatic lung tumors derived from thyroid carcinoma (n=12), oral floor carcinoma (n=4), esophageal carcinoma (n=4), malignant thymoma (n=2), laryngeal carcinoma (n=1) and sigmoid colon carcinoma (n=1). Benign lesions consisted of organizing inflammatory nodules (n=5) and a sclerosing hemangioma (n=1). The mean ±SD of the maximum diameter of the lesions was 1.7±0.9 cm (range: 0.4-4.5 cm). Lesions were located in the lower lung field (n=21), middle lung field (n=10) and upper lung field (n=1). The mean±SD of the vital capacity (VC) was 3.1±0.7 L (range: 2.0-4.3 L), that of the percent forced expiratory volume in 1 second (%$FEV_{1.0}$) was 71.7 ±8.1% (range: 51.4-96.5%) and that of the body mass index (BMI) was 22.4±3.3 (range: 17.0-31.4). The percentage of VC was within the normal range in all patients (%VC > 80%).

Data acquisition and image reconstruction

All PET/CT examinations were performed using a Discovery STE scanner (GE Healthcare, Milwaukee, WI, USA). The detector of this scanner was composed of bismuth germinate ($B_4G_3O_{12}$) crystal. The intrinsic resolution was 5.3 mm of full width at half maximum (FWHM). The PET data was acquired in the 3D mode with a 128×128 matrix (5.47×5.47×3.2 mm). The sensitivity of the PET scanner was 9.0 kcps/kBq. The 16-slice CT scanning was performed in the helical mode using the following parameters: 120 kV, auto mA, matrix 512×512, slice thickness 5 mm, rotation time 0.5 seconds/rotation. The PET/CT images were reconstructed using a 3D-ordered subsets-expectation maximization (3D-OSEM) algorithm (VUE Point Plus), with 2 iterations, 28 subsets and a post-filter of 6 mm of FWHM.

All patients fasted for at least 4 hours before PET/CT examination. They were intravenously injected with 141.2-307.6 MBq of FDG. After a whole body CT scan with free breathing (FB-CT) was performed, a whole body FB-PET scan was started 60 minutes after the FDG injection. Both the FB-CT and FB-PET examinations were performed with free shallow breathing. A whole-body FB-PET scan from head to thigh was performed for 3 minutes per bed position. When lung lesions were found in the FB-PET/CT examination, a BH examination of the thorax immediately followed. The BH-CT was performed with deep inspiration, and this was followed by 5 BH-PET scans with deep inspiration for 20 seconds each (BH1-BH5). Patients rested with free breathing for 15 seconds after each BH-PET scan. BH×1 was a single BH scan with the smallest displacement between PET and CT images among BH1-BH5. The average displacement among the BH1-BH5 scans was expressed as the BHmean. BH images with total acquisition times of 40, 60, 80 and 100 seconds were generated by the summation of 2, 3, 4 and 5 BH images, respectively (BH×2, BH×3, BH×4 and BH×5).

Measurement of the displacement between PET and CT images

PET/CT images were analyzed using a workstation (Eclipse; Varian Medical Systems, Palo Alto, CA). This workstation is normally used for radiotherapy planning. The tumor outline on the CT image was determined by manually tracing the tumor border seen in a lung window display (width: 2000, level: 250). The tumor outline on a PET image was first extracted by auto contouring with 27% of SUVmax [29], and finally determined after modification by a board certified nuclear medicine physician referring to his visual assessment. The center of the tumor (X, Y, Z) was automatically determined following the determination of the tumor outline. The displacement between PET and CT images was calculated using the following formula:

$$\text{Displacement (cm)} = [(X_{CT} - X_{PET})^2 + (Y_{CT} - Y_{PET})^2 + (Z_{CT} - Z_{PET})^2]^{0.5}$$

where X is the lateral direction, Y is the ventrodorsal direction and Z is the craniocaudal direction. The center of the tumor in the BH-PET scans was compared with that in the BH-CT scans, while that in the FB-PET scans was compared with that in the FB-CT scans.

Analysis of image quality and SUVmax

To evaluate the image quality, square regions of interest (ROIs) with 9×9 pixels were placed on both the lesion and the contralateral normal lung field in the same slice. The contrast, coefficient of variance (CV) and signal-to-noise ratio (SNR) were then calculated using the following formula:

$$\text{Contrast} = (L_{max} - N_{mean}) / (L_{max} + N_{mean})$$

$$CV = \sigma / N_{mean} \times 100$$

$$SNR = (L_{max} - N_{mean}) / \sigma$$

where L_{max} is the maximum count of the lesion, N_{mean} is the mean count of the normal lung field, and σ is the standard deviation of the count in the normal lung field. The SUVmax represents the maximum SUV value of the single pixel in the lesion.

Visual assessment of image quality was performed by three board certified nuclear medicine physicians independently. The image quality was scored by using the following five point scale: 5, excellent image quality; 4, sufficient image quality for diagnosis; 3, possibly sufficient image quality for diagnosis; 2, poor image quality for diagnosis; 1, unacceptable image quality for diagnosis. The visual score was acquired by averaging the results of three observer's score. An image with a score of 3 or higher was considered to be suitable for diagnosis.

Statistical analysis

The nonparametric Mann-Whitney U test was applied to evaluate the relationship between the displacement and the clinical features of the patient (age, VC, BMI and $\%FEV_{1.0}$). Multiple comparisons of the displacement, SUVmax, tumor volume, contrast, CV and SNR among the BH images and FB image were performed using the Tukey–Kramer method. A p value < 0.05 was considered to be significant.

Results

All of 32 lesions were positive on FDG-PET images of FB and all BH images. The tumor volume, displacement and SUVmax are summarized in Table 1. The tumor volume and the displacement in the BH scan were significantly smaller than those in the FB scan ($P<0.01$), but were slightly increased with an increasing summation number.

We compared the displacement among the 5 BH scans (Fig. 1). The mean displacement and variability increased in later BH scans (Fig. 1A), however, the displacement of many lesions was less than 5 mm (Fig. 1B). Large displacements were observed in less than one-third of the patients (28%, 9 out of 32 lesions).

Table 2 shows the relationship between the patient characteristics and the displacement of the BH scan. The mean displacement among 5 BH scans was significantly larger in patients who were 60 years old or older and whose %$FEV_{1.0}$ was 70% or less. In patients whose VC was 3 L or less, the displacement was relatively large, but the difference was not significant. The SUVmax was significantly increased in the BH scans ($P<0.01$) but was decreased slightly with an increasing summation number (Table 1). Figure 2 shows an example of FB- and BH-PET/CT images of one patient. The BH×5-PET/CT images show a decreased tumor volume, improved registration and increased SUVmax compared to the FB-PET/CT images.

The results of the image quality are shown in Table 1. The contrast of the BH images was superior to that of the FB images ($P<0.01$). However, the summation of the BH images did not improve the contrast. The CV of the BH images was inferior to that of the FB images ($P<0.01$). The summation of the BH images improved the CV by increasing the number of images summed. In comparison to the BH×5, the CV of

BH×1~BH×3 was significantly inferior ($P<0.01$), while that of BH×4 was not significantly different. The SNR of the BH images was superior to that of the FB images ($P<0.01$), and the summation of the BH images showed an improvement in the SNR. The SNR of BH×5 was significantly superior to that of both BH×1 and BH×2 ($P<0.01$).

The results of the visual assessment of image quality are shown in Table 1. In the BH scan, the score increased with an increasing summation number. To obtain a score of 3 or more, at least 3 BH images (total acquisition time of 60 seconds) had to be summed. Figure 3 shows both the FB- and summed BH-PET images. Although small lung tumor could be clinically observed in all PET images, good image quality was achieved only in BH×3, BH×4 and BH×5 images.

Discussion

In this study, we evaluated the image quality of BH-PET/CT for diagnosing thoracic lesions, and determined the optimal acquisition protocol for BH-PET/CT. BH scanning minimized the misregistration and increased the SUVmax compared with FB scanning. Because the short acquisition time of BH imaging resulted in a degraded image quality, use of a summation of 3 or more BH images (total acquisition time of 60 seconds or more) is recommended to obtain good image quality for clinical use.

The displacement between PET and CT images and the tumor volume were significantly decreased in the BH-PET/CT because of the elimination of tumor blurring. BH-PET images also showed significant increase in the SUVmax compared with FB-PET images. Preventing smearing of a lesion's radioactivity by BH scanning resulted an increase in the SUVmax. Improvement of the registration between PET and CT images must provide effective attenuation correction to obtain the true SUV. The contrast and SNR of the BH images was superior to that of the FB images. In addition to the increased SUVmax of lesions, the decreased background radioactivity reinforced these results. Because the BH scan was performed under deep inspiration status, the radioactivity in the lung field was decreased in the widely expanded lung [22]. On the other hand, the CV of FB images was superior to that of BH images. Because the CV is dependent on the statistical variance of the acquired count, the CV is therefore highly influenced by the acquisition time.

Some authors have examined the optimal acquisition time of BH-PET in phantom studies [26-28]. Yamaguchi et al. proposed at least a 45-second breath-hold, because the detectability was not significantly different from that of a 120-second acquisition [26]. Tsuda et al. recommended at least 90 seconds in the low lesion to background radioactivity ratio (LB ratio=4) [28]. On the other hand, Miyashita et al.

observed that the relative error of CV with 90-second acquisition was within 20% of that with 120-second acquisition when using a homogeneous cylindrical phantom [27].

In a clinical study, some reports proposed a BH-PET scanning with an acquisition time of 9×20 seconds, which was equal to that of a FB scan [23, 24] Miyashita et al. performed 8×12-second acquisitions for BH scans (total acquisition time of 96 seconds) [27], while Kawano et al. employed the list-mode dynamic collection method and acquired the data as long as patients could hold their breath. The acquisition time of their BH scans varied considerably, ranging from 30 to 125 seconds [22]. Although the usefulness of BH-PET/CT has been reported, the necessity of a long acquisition time would not be acceptable for either uncooperative or sick patients. A previous study reported that a breath holding was not acceptable for older patients with underlying lung disease such as emphysema or pulmonary fibrosis [21]. They also reported that 15-20% of the patients failed to hold their breath in the same respiratory phase as for the CT acquisition.

A short acquisition time is normally desirable for patients with a lung lesion. A single 20-second acquisition of a BH scan was reported by Torizuka et al [21]. Nagamachi et al. performed 4 BH-PET scans of 30 second acquisitions and minimized the variance by averaging the scans [20]. However, our results suggested that the image quality of a single 20- or 30-second acquisition was not sufficient for clinical use. Besides, the increase of the SUVmax in the short acquisition time may have been related to an increase in noise. Although Torizuka et al. concluded that the single 20-second acquisition time of BH-PET enabled precise measurement of SUVmax [21], they did not consider the effect of increased noise on the SUVmax measurement. In our study, the SUVmax was decreased by increasing the summation number. Therefore, the BH-PET with a short acquisition time might not be of good enough quality to evaluate the precise SUVmax for differentiating between malignant or benign tumors or for monitoring the therapeutic response of tumors.

Our results suggested that the number of BH images for summation should be 4 or more based on the CV, and 3 or more based on the SNR. Furthermore, the results of visual assessment suggested that 3 or more BH images for summation was required to obtain good image quality for interpretation. According to these findings, we considered that 3 or more 20-second BH-PET scans should be summed, thus resulting in a total acquisition time of 60 seconds or more, in order to provide sufficient image quality.

A large displacement was not dependent on the order of the BH scan, but was observed in a limited number of patients. The relationship between the patient clinical characteristics and the displacement in the BH scans showed that the displacement was significantly higher in patients aged 60 years old or older and with a % $FEV_{1.0}$ of less than 70%, and it tended to be higher in patients with less than 3 L of VC. Thus, the reproducibility of BH-PET/CT images is considered to depend on both patient age and lung function. The real-time position management system (RPM) and visual feedback-guided breath-hold technique achieved good reproducibility of BH in radiotherapy [13, 14]. The monitoring of the respiratory motion to guide a patient's respiration may therefore improve the reproducibility of BH-PET/CT imaging.

The present study had some limitations. First, the optimal acquisition time of BH-PET is considered to depend on the PET device, the size of the matrix, the method of reconstruction and the parameters for reconstruction. Therefore, the optimal acquisition time should be determined at each institution. Second, the visual assessment was performed for only image quality. To evaluate the usefulness of our protocol, an examination to assess the detectability of lesions is required.

Developments in PET/CT devices, reconstruction methods and correction methods have enabled clinicians to obtain good quality images using protocols with short acquisition times [30-33]. Shortening the total acquisition time of BH scans is promising to ease the burden for patients. Furthermore, the short acquisition time can increase the number of bed positions, resulting in a wide range of possible BH-PET scans. Extending the scanning range of BH-PET/CT is expected to be useful for both tumor staging and the detection of recurrent tumors [25].

In conclusion, BH-PET/CT improved the registration between PET and CT images and increased the SUVmax of thoracic lesions. Based on the evaluation of image quality, the recommended number of BH-PET images for summation with 20 seconds of acquisition time is 3 or more. Further examination is recommended to assess the diagnostic accuracy using this acquisition protocol.

Acknowledgements

The authors thank the staff of the Department of Clinical Radiology and Medical Technology at Kyushu University Hospital for their valuable clinical support, and we also thank Mr. Tatsuya Mitsumoto (GE Healthcare Japan) for his technical assistance. This study was supported in part by a Grant-in Aid for Scientific Research © from the Japan Society for the Promotion of Science KAKENHI (No. 22611012).

References

1 Gould MK, Maclean CC, Kuschner WG, Rydzak CE, Owens DK. Accuracy of positron emission tomography for diagnosis of pulmonary nodules and mass lesions: A meta-analysis. *JAMA* 2001; **285**:914-924.

2 Hicks RJ, Kalff V, MacManus MP, et al. The utility of ^{18}F-FDG PET for suspected recurrent non-small cell lung cancer after potentially curative therapy: Impact on management and prognostic stratification. *J Nucl Med* 2001; **42**:1605-1613.

3 Oyen WJ, Bussink J, Verhagen AF, Corstens FH, Bootsma GP. Role of FDG-PET in the diagnosis and management of lung cancer. *Expert Rev Anticancer Ther* 2004; **4**:561-567.

4 Vansteenkiste J, Fischer BM, Dooms C, Mortensen J. Positron-emission tomography in prognostic and therapeutic assessment of lung cancer: Systematic review. *Lancet Oncol* 2004; **5**:531-540.

5 Dwamena BA, Sonnad SS, Angobaldo JO, Wahl RL. Metastases from non-small cell lung cancer: Mediastinal staging in the 1990s--meta-analytic comparison of PET and CT. *Radiology* 1999; **213**:530-536.

6 Beyer T, Townsend DW, Brun T, et al. A combined PET/CT scanner for clinical oncology. *J Nucl Med* 2000; **41**:1369-1379.

7 Cerfolio RJ, Ojha B, Bryant AS, Raghuveer V, Mountz JM, Bartolucci AA. The accuracy of integrated PET-CT compared with dedicated PET alone for the staging of patients with nonsmall cell lung cancer. *Ann Thorac Surg* 2004; **78**:1017-23; discussion 1017-23.

8 Cohade C, Osman M, Marshall LN, Wahl RN. PET-CT: Accuracy of PET and CT spatial registration of lung lesions. *Eur J Nucl Med Mol Imaging* 2003; **30**:721-726.

9 Erdi YE, Nehmeh SA, Pan T, et al. The CT motion quantitation of lung lesions and its impact on PET-measured SUVs. *J Nucl Med* 2004; **45**:1287-1292.

10 Hickeson M, Yun M, Matthies A, et al. Use of a corrected standardized uptake value based on the lesion size on CT permits accurate characterization of lung nodules on FDG-PET. *Eur J Nucl Med Mol Imaging* 2002; **29**:1639-1647.

11 Yu J, Li X, Xing L, et al. Comparison of tumor volumes as determined by pathologic examination and FDG-PET/CT images of non-small-cell lung cancer: A pilot study. *Int J Radiat Oncol Biol Phys* 2009; **75**:1468-1474.

12 Wulf J, Haedinger U, Oppitz U, Thiele W, Mueller G, Flentje M. Stereotactic radiotherapy for primary lung cancer and pulmonary metastases: A noninvasive treatment approach in medically inoperable patients. *Int J Radiat Oncol Biol Phys* 2004; **60**:186-196.

13 Yoshitake T, Shioyama Y, Nakamura K, et al. A clinical evaluation of visual feedback-guided breath-hold reproducibility of tumor location. *Phys Med Biol* 2009; **54**:7171-7182.

14 Berson AM, Emery R, Rodriguez L, et al. Clinical experience using respiratory gated radiation therapy: Comparison of free-breathing and breath-hold techniques. *Int J Radiat Oncol Biol Phys* 2004; **60**:419-426.

15 Gregoire V, Haustermans K, Geets X, Roels S, Lonneux M. PET-based treatment planning in radiotherapy: A new standard? *J Nucl Med* 2007; **48** Suppl 1:68S-77S.

16 Nehmeh SA, Erdi YE, Pan T, et al. Four-dimensional (4D) PET/CT imaging of the thorax. *Med Phys* 2004; **31**:3179-3186.

17 Pan T, Lee TY, Rietzel E, Chen GT. 4D-CT imaging of a volume influenced by respiratory motion on multi-slice CT. *Med Phys* 2004; **31**:333-340.

18 Halpern BS, Dahlbom M, Quon A, et al. Impact of patient weight and emission scan duration on PET/CT image quality and lesion detectability. *J Nucl Med* 2004; **45**:797-801.

19 Macdonald LR, Schmitz RE, Alessio AM, et al. Measured count-rate performance of the discovery STE PET/CT scanner in 2D, 3D and partial collimation acquisition modes. *Phys Med Biol* 2008; **53**:3723-3738.

20 Nagamachi S, Wakamatsu H, Kiyohara S, et al. The reproducibility of deep-inspiration breath-hold ^{18}F-FDG PET/CT technique in diagnosing various cancers affected by respiratory motion. *Ann Nucl Med* 2010; **24**:171-178.

21 Torizuka T, Tanizaki Y, Kanno T, et al. Single 20-second acquisition of deep-inspiration breath-hold PET/CT: Clinical feasibility for lung cancer. *J Nucl Med* 2009; **50**:1579-1584.

22 Kawano T, Ohtake E, Inoue T. Deep-inspiration breath-hold PET/CT of lung cancer: Maximum standardized uptake value analysis of 108 patients. *J Nucl Med* 2008; **49**:1223-1231.

23 Nehmeh SA, Erdi YE, Meirelles GS, et al. Deep-inspiration breath-hold PET/CT of the thorax. *J Nucl Med* 2007; **48**:22-26.

24 Meirelles GS, Erdi YE, Nehmeh SA, et al. Deep-inspiration breath-hold PET/CT: Clinical findings with a new technique for detection and characterization of thoracic lesions. *J Nucl Med* 2007; **48**:712-719.

25 Daisaki H, Shinohara H, Terauchi T, et al. Multi-bed-position acquisition technique for deep inspiration breath-hold PET/CT: A preliminary result for pulmonary lesions. *Ann Nucl Med* 2010; **24**:179-188.

26 Yamaguchi T, Ueda O, Hara H, et al. Usefulness of a breath-holding acquisition method in PET/CT for pulmonary lesions. *Ann Nucl Med* 2009; **23**:65-71.

27 Miyashita K, Tateishi U, Nishiyama Y, Minamimoto R, Shizukuishi K, Inoue T. Optimal emission time in deep-inspiration breath-hold PET-CT: A preliminary result. *Ann Nucl Med* 2010; **24**:559-563.

28 Tsuda K, Sasaki T, Iwabuchi Y, et, al. Evaluation of an experimental breath-holding image acquisition with regard to pulmonary nodule detection on chest FDG PET image. *Radioisotopes* 2010; **59**:587-598

29 Zhang T, Tachiya Y, Sakaguchi Y, et al. Phantom study on three-dimensional target volume delineation by PET/CT-based auto-contouring. *Fukuoka Igaku Zasshi* 2010; **101**:238-246.

30 Brambilla M, Secco C, Dominietto M, Matheoud R, Sacchetti G, Inglese E. Performance characteristics obtained for a new 3-dimensional lutetium oxyorthosilicate-based whole-body PET/CT scanner with the national electrical manufacturers association NU 2-2001 standard. *J Nucl Med* 2005; **46**:2083-2091.

31 Chatziioannou AF, Cherry SR, Shao Y, et al. Performance evaluation of microPET: A high-resolution lutetium oxyorthosilicate PET scanner for animal imaging. *J Nucl Med* 1999; **40**:1164-1175.

32 Karp JS, Surti S, Daube-Witherspoon ME, Muehllehner G. Benefit of time-of-flight in PET: Experimental and clinical results. *J Nucl Med* 2008; **49**:462-470.

33 Kadrmas DJ, Casey ME, Conti M, Jakoby BW, Lois C, Townsend DW. Impact of time-of-flight on PET tumor detection. *J Nucl Med* 2009; **50**:1315-1323.

Legends for Figures

Figure 1. A comparison of the displacement among 5 BH-PET images (BH1~BH5). The mean displacement was not significantly different among the scans, but there was high variability (A). The displacement of all lesions is shown in (B). Although the displacement of most lesions was less than 0.5 cm, high variability was observed in a limited number of patients.

Figure 2. A 37-year-old female with multiple lung metastases from an oral floor carcinoma. The biggest tumor, with a diameter of 2.15 cm, was in the left lower lobe of the lung. Transaxial, sagittal and coronal images of FB-PET/CT (A) and BH×5-PET/CT (B) are shown. The BH-PET/CT image is a summation of 5 BH images. The displacement between the tumor in PET and that in CT was 1.90 cm in FB-PET/CT and 0.10 cm in BH×5 PET/CT. The SUVmax was 9.29 and 12.54, and the tumor volume was 4.67cm^3 and 4.10cm^3 in FB- and BH-PET/CT, respectively.

Figure 3. A 64-year-old female with lung metastasis from thyroid carcinoma. A tumor with a diameter of 1.41 cm was located in the right lower lobe. FB-PET showed a score of 4 and a CV of 27.1. Both BH×1 and BH×2 showed poor image quality (score: 2 and 2.67; CV: 55.6 and 45.0, respectively). BH×3, BH×4 and BH×5 showed relatively good image quality (score: 3.33, 3.67 and 3.67; CV: 36.3, 36.7 and 34.3, respectively).

figure 1

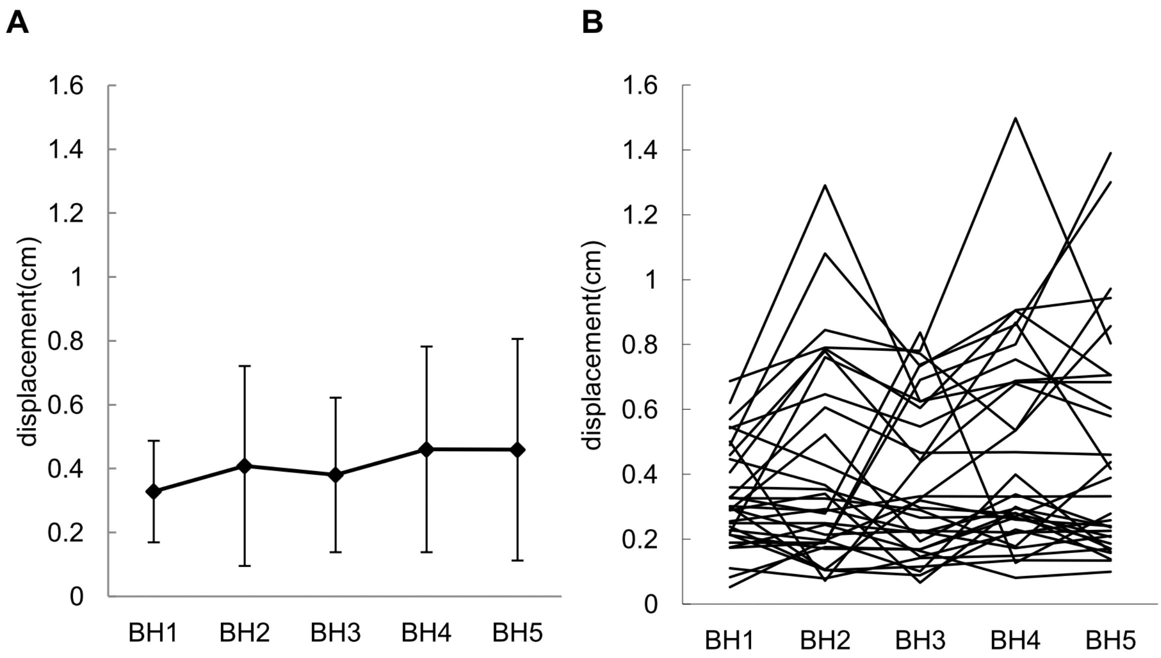
A
B
1.6
1.4
1.2
1
0.8
0.6
0.4
0.2
0
displacement(cm)
BH1
BH2
BH3
BH4
BH5
1.6
1.4
1.2
1
0.8
0.6
0.4
0.2
0
displacement(cm)
BH1
BH2
BH3
BH4
BH5

figure 2

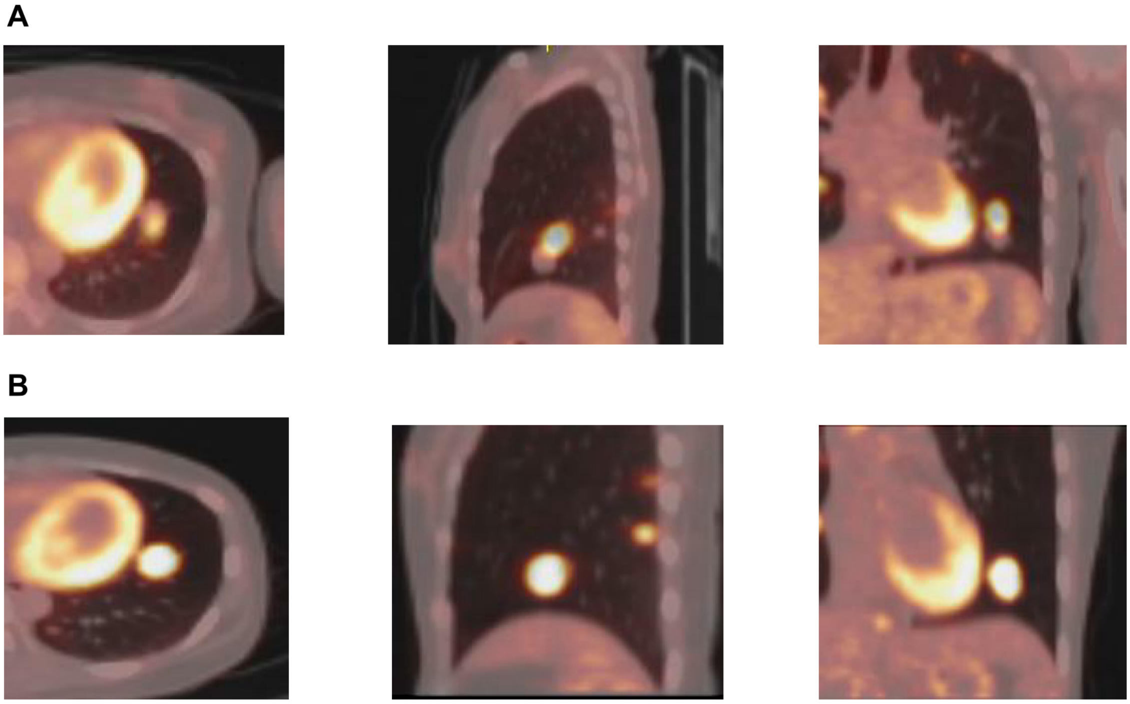

figure 3